C_{60}-Fullerene Monomalonate Adducts Selectively Inactivate Neuronal Nitric Oxide Synthase by Uncoupling the Formation of Reactive Oxygen Intermediates from Nitric Oxide Production†

Donald J. Wolff,*,‡ Krystian Mialkowski,‡ Christine F. Richardson,§ and Stephen R. Wilson§

Department of Pharmacology, University of Medicine and Dentistry of New Jersey, Robert Wood Johnson Medical School, Piscataway, New Jersey 08854, and Department of Chemistry, New York University, New York, New York 10003

Received August 16, 2000; Revised Manuscript Received November 2, 2000

ABSTRACT: C_{60}-Fullerene monomalonate adducts inactivate selectively the neuronal nitric oxide synthase isoform in a manner completely preventable by the concurrent presence of superoxide dismutase and catalase. This inactivation is time-, fullerene concentration-, and turnover-dependent and is not reversible by dilution. The di(carboxypropan-3-ol)methano-[60]-fullerene (diol adduct) has no effect on NADPH consumption by nNOS as measured in the absence of arginine substrate, but dramatically increases NADPH consumption in the presence of arginine. This fullerene-enhanced NADPH consumption is linked to oxygen as electron acceptor and is accompanied by the increased production of hydrogen peroxide. These effects of fullerene monomalonate adducts are unique to the nNOS isoform and are not observed using either the iNOS or the eNOS isoform. The inhibitory effects of fullerene monomalonate adducts are unaltered and insurmountable by increased concentrations of arginine, tetrahydrobiopterin, or calmodulin. These observations indicate that fullerene monomalonate adducts uncouple in the presence of arginine the formation of reactive oxygen intermediates from NO production by nNOS. These reactive oxygen intermediates dissociate from the enzyme and, acting from solution, inactivate NOS NO forming activity.

Nitric oxide (NO)[1] is a widespread and important regulatory substance in mammalian physiology (*1*). Nitric oxide serves as a neurotransmitter in the central and peripheral nervous systems (*2*), is a regulator of blood pressure and blood flow (*3*), and provides defense against foreign organisms in the nonspecific efferent arm of the immune system (*4*). NO is synthesized by nitric oxide synthase (NOS), a cytochrome P450-like heme protein that utilizes tetrahydrobiopterin, FAD, and FMN as cofactors to catalyze the NADPH-dependent oxidation of L-arginine to form citrulline and NO (*5, 6*). Nitric oxide synthase exists in three major isozymic forms (*7*): a constitutive, Ca^{2+}- and calmodulin (CaM)-dependent form (nNOS, form I) isolated from neurons and GH_3 pituitary cells (*8*); a cytokine-inducible isoform (iNOS, form II) distributed widely and characterized extensively from macrophages (*9, 10*); and a constitutive, Ca^{2+}- and CaM-dependent isoform (eNOS, form III) isolated from endothelia (*11*).

In particular circumstances, NO synthesis can be excessive and may lead to cytotoxic outcomes. Overproduction of NO by the cytokine-inducible isoform has been implicated in the pathogenesis of septic shock (*12*) and in diverse autoimmune disorders such as multiple sclerosis (*13*) and arthritis (*14*). Overproduction of NO by the neuronal NOS isoform has been implicated in the tissue damage accompanying ischemia−reperfusion following stroke (*15*) and in diverse neurodegenerative disorders (*16*). Accordingly, many laboratories have directed their attention to the development and characterization of NOS inhibitors selective for the iNOS or nNOS isoform but that spare the eNOS isoform necessary for the maintenance of appropriate tissue blood flow.

Fullerenes, a class of spheroidally shaped molecules, composed entirely of carbon atoms, were initially reported in 1985 (*17*) and are now preparable in quantities sufficient to examine their biological activities (*18*). The principal obstacle to progress in this endeavor is their almost total absence of water solubility. Fullerenes can now be functionally substituted with water-solubilizing addends of diverse structure attached in geometrically diverse arrays (*19*−*21*). Such fullerene adducts have been identified as inhibitors of cysteine (*22*) and serine (*23*) proteinases, exhibit HIV antiviral activity (*24*−*26*), and confer protection against glutamate-induced neurotoxicity in vitro and in vivo (*27, 28*). Recently our laboratory (*29*) has reported that the C_3 and

† This work was supported at UMDNJ by National Institutes of Health Grants ES 06897 and HL 54768.

* Corresponding author. Telephone: 732-235-4083. Fax: 732-235-4073. E mail: wolffdj@umdnj.edu.

‡ Robert Wood Johnson Medical School.

§ New York University.

[1] Abbreviations: NO, nitric oxide; NOS, nitric oxide synthase; diol adduct, di(carboxypropan-3-ol)methano-[60]-fullerene; semi-amine adduct, (ethoxycarbonylcarboxypropan-3-amino)methano-[60]-fullerene; diamine adduct, di(carboxypropan-3-amino)methano-[60]-fullerene; DBU, 1,8-diazobicyclo[5.4.0]undec-7-ene; DMSO, dimethyl sulfoxide; Mops, 4-morpholinepropanesulfonic acid; EGTA, ethylene glycol bis-(β-aminoethyl ether)-*N*,*N*,*N*′,*N*′-tetraacetic acid; DTT, dithiothreitol; CHAPSO, 3-[(3-cholamidopropyl)dimethylammonio]-2-hydroxy-1-propanesulfonic acid; BH_4, (6*R*)-5,6,7,8-tetrahydro-L-biopterin; iNOS, inducible nitric oxide synthase; nNOS, neuronal nitric oxide synthase; eNOS, endothelial nitric oxide synthase; DMEM, Dulbecco's modified Eagle's medium; Hepes, *N*-(2-hydroxyethyl)piperazine-*N*′-2-ethanesulfonic acid; CaM, calmodulin.

10.1021/bi0019444 CCC: $20.00
Published on Web 12/09/2000

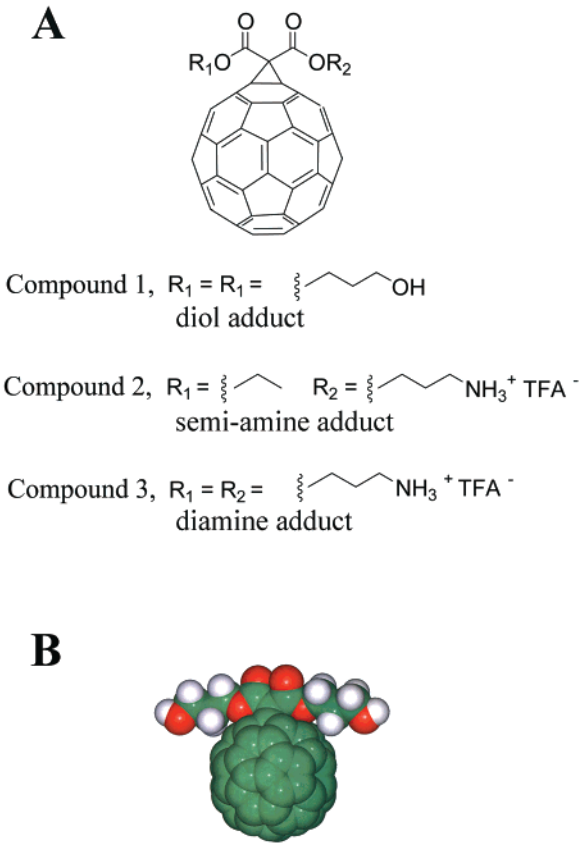

FIGURE 1: Panel A: Structure and informal nomenclature of the three fullerene monomalonate adducts used in this study. Panel B: Three-dimensional model of the diol adduct.

D_3 regioisomers of C_{60}-fullerene trisubstituted with malonate groups inhibit reversibly NO formation by all three NOS isoforms. These inhibitions displayed only a 3-fold isoform selectivity and exhibited relatively low potency. Accordingly, our laboratory was interested in extending these initial observations by examining the effects of altering the degree of, the positioning of, and the chemical nature of adduction on the properties of fullerenes as NOS inhibitors. We report here that several monoadducted fullerenes selectively inactivate the neuronal NOS isoforms by uncoupling in the presence of arginine the formation of reactive oxygen intermediates from NO and citrulline formation.

EXPERIMENTAL PROCEDURES

Materials. Hydrogen peroxide, ferrous ammonium sulfate, and sodium thiocyanate were obtained from Sigma. All other reagents were obtained as described previously (*30*).

Preparation and Characterization of Water-Soluble Fullerene Derivatives. Following general procedures from Hirsch and co-workers (*31*), three new monomalonate adducts of C_{60} were prepared (for structures, see Figure 1). Fullerene adducts were prepared using a three-step synthetic scheme. Initially, malonate esters containing appropriately protected alcohol and amine residues are prepared. These malonate esters are then coupled to the C_{60}-fullerene. The coupled aminofullerenes were deprotected with a trifluoroacetic acid solution, and the protected alcohol was deprotected with *p*-toluenesulfonic acid as described previously (*21*).

*Synthesis and Characterization of Compound **3**, the Diamine Fullerene Adduct.* The diamine adduct was prepared and characterized exactly as described previously (*21*).

*Synthesis and Charcterization of Compound **1**, the Diol Fullerene Adduct. (A) Synthesis of Di[3-(tert-butyldimethylsilanyloxy)propyl]malonate.* To a solution of 5 g (0.03 mol) of 3-(*tert*-butyldimethylsilanyloxy)-1-propanol in 200 mL of dry methylene chloride under nitrogen was added 2.08 g (0.03 mol) of pyridine. To this was added 1.85 g (0.01 mol) of freshly distilled malonyl dichloride. The resulting solution was allowed to stir at room temperature for 2 h, at which time the reaction was stopped. Then 100 mL of saturated sodium bicarbonate was added, and the mixture was extracted into 3 × 100 mL of ether. The ether extracts were combined, dried over anhydrous sodium sulfate, and evaporated. The crude reaction mixture was separated on a silica gel column using 25% ethyl ether/hexane as the eluent [% yield 49%; mass calculated for $C_{21}H_{44}O_6Si_2$ 448, mass spectrometry found 448; ^{1}H NMR (200 MHz, $CDCl_3$) δ 0.01 (s), 0.86 (s), 1.81 (m), 3.32 (s), 3.65 (t), 4.21 (t); ^{13}C NMR (200 MHz, $CDCl_3$) δ −4.83, 18.82, 26.44, 32.21, 42.10, 59.72, 63.02, 166.81; R_f = 0.6, silica gel, 25% ethyl ether/hexane].

(B) Coupling of Di[3-(tert-butyldimethylsilanyloxy)propyl]-malonate to C_{60}-Fullerene. To a solution of 1 g (1 equiv) of C_{60} and 691 mg (1.5 equiv) of carbon tetrabromide (CBr_4) in 500 mL of toluene was added 933 mg (1.5 equiv) of di-[3-(*tert*-butyldimethylsilanyloxy)propyl]malonate followed by 634 mg (3 equiv) of 1,8-diazobicyclo[5.4.0]undec-7-ene (DBU). The mixture was allowed to stir for 30 min, at which time the product was observed on TLC. The crude reaction mixture was washed with water (3 × 100 mL), dried over anhydrous sodium sulfate, and evaporated. The product was separated on a silica gel column using 1:1 hexane/toluene as eluent to remove unreacted C_{60} followed by toluene to elute the monoadduct [% yield based on recovered C_{60} 47.3%; R_f = 0.64, silica gel, 100:1 toluene/ethyl acetate; ^{1}H NMR (200 MHz, $CDCl_3$) δ 0.09 (s), 0.92 (s), 2.03 (m), 3.78 (t), 4.5 (t); ^{3}He NMR (500 MHz, methylnaphthalene/dCH_2Cl_2 3:1) δ −8.006; mass calculated for $C_{69}H_{14}O_6$ 938, found 937.7].

*Synthesis and Characterization of Compound **2**, the Semi-amine Fullerene Adduct. (A) Synthesis of [Ethyl-3-tert-butoxycarbonylaminopropyl]malonate.* To a solution of 5 g (0.03 mol) of *tert*-butyl *N*-(3-hydroxypropyl)carbamate in 200 mL of dry methylene chloride under an inert atmosphere was added 2.29 g (0.03 mol) of pyridine. To this was added 4.36 g (0.03 mol) of ethyl malonyl chloride. The mixture was allowed to stir overnight. Then 100 mL of saturated sodium bicarbonate was added, and the mixture was extracted with 3 × 100 mL of diethyl ether. The ether extracts were combined, dried over anhydrous sodium sulfate, and evaporated. The mixture was separated on a silica gel column using 25% ethyl ether/hexane as eluent [% yield 84%; mass calculated for $C_{13}H_{23}O_6N$ 290, mass spectrometry found 290; ^{1}H NMR (200 MHz, $CDCl_3$) δ 1.30 (t), 1.43 (s), 1.80 (m), 3.12 (q), 3.37 (s), 4.18 (m), 4.80 (bs); ^{13}C NMR (200 MHz, $CDCl_3$) δ 168.82, 166.8, 156.33, 79.84, 63.56, 62.13, 42.02, 38.13, 29.60, 29.98, 28.48, 28.15, 14.67].

(B) Coupling of [Ethyl-3-tert-butoxycarbonylaminopropyl]-malonate to C_{60}-Fullerene. To a solution of 5 g (1 equiv) of C_{60} and 3.45 g (1.5 equiv) of CBr_4 in 3 L of toluene was added 3 g (1.5 equiv) of malonate followed by 3.1 g (3 equiv)

of DBU. The mixture was allowed to stir at room temperature for 30 min, at which time the product was visible on TLC. The reaction mixture was washed in two portions of approximately 1.5 L each with water (3 × 1 L), dried over anhydrous sodium sulfate, and evaporated. Each portion was separated on a silica gel column using toluene to remove unreacted C_{60} and 10:1 toluene/ethyl acetate to remove the product [% yield based on recovered C_{60} 73.1%; $R_f = 0.56$, silica gel, 10:1 toluene/ethyl acetate; ^{1}H NMR (300 MHz, $CDCl_3$) δ 1.71 (s), 1.74 (t), 2.31 (m), 3.59 (q), 4.84 (m), 5.07 (bs); mass calculated for $C_{73}H_{21}O_6N$ 1.007.17, mass spectrometry found 1008; ^{3}He NMR (500 MHz, methylnaphthalene/dCH_2Cl_2 3:1) δ −8.055].

The ^{3}He NMR spectra obtained for each of the monomalonate adducts of C_{60} prepared as described above were exactly as expected for a monoderivatized fullerene as based on previously published observations (*32*−*35*). Each of the monomalonate adducts was found to be soluble in dimethyl sulfoxide at concentrations up to 10 mM. Aqueous solutions were prepared by dilution of the DMSO stock in water. The DMSO carried into enzyme solutions from the stock was found in control experiments to have no effect on activity at the concentrations delivered.

Purification of Neuronal NOS. Neuronal NOS was purified from rat GH_3 pituitary cells grown in Ham's F-10 supplemented with 12.5% horse serum and 3% fetal bovine serum. Cells were homogenized in 5 volumes of 50 mM Mops, pH 7.4, 1 mM EGTA, 1 mM DTT, 100 mM NaCl, 0.5% CHAPSO, 50 μM BH_4, 100 μM leupeptin, and 10 μM E64. A postmitochondrial supernatant fraction was generated by centrifugation and was affinity-purified on 2′,5′-ADP−agarose as reported previously (*8*). The affinity-purified proteins were eluted with 50 mM Mops, pH 7.4, 1 mM EGTA, 1 mM DTT, 5 mM NADPH, 0.1% CHAPSO, 150 mM NaCl, 50 μM BH_4, 100 μM leupeptin, and 10 μM E64. The eluate was adjusted to contain 2.5 mM Ca^{2+} and was adsorbed to a calmodulin-Affi Gel 15 agarose column equilibrated in 50 mM Mops, 1 mM EGTA, 2.5 mM Ca^{2+}, 0.1% CHAPSO, 150 mM NaCl, 25 μM arginine, 1 mM DTT, 50 μM BH_4, 100 μM leupeptin, and 10 μM E64. The column was washed with equilibration buffer containing 500 mM NaCl but without arginine, and nNOS was eluted with equilibration buffer containing 2.5 mM EGTA but without Ca^{2+} or arginine. Fractions containing nNOS as determined by the citrulline formation assay were concentrated with a Centriprep 30 (Amicon). Purified nNOS displayed a single band on a Coomassie blue-stained SDS−PAGE and catalyzed formation of 0.47 μmol of citrulline min^{-1} (mg of protein)$^{-1}$as determined at saturating L-arginine and BH_4 concentrations.

Purification of iNOS. Cytokine-inducible NOS was purified from murine RAW 264.7 macrophages grown in DMEM/Hepes, pH 7.5, supplemented with 10% fetal bovine serum. Expression of iNOS was induced with 5 μg/mL *Escherichia coli* lipopolysaccharide and 50 units/mL mouse γ-interferon. Homogeneous preparation of the iNOS was obtained through sequential purification on 2′,5′-ADP−agarose and DEAE-cellulose as described previously (*36*). Purified iNOS was about 95% pure as judged by a Coomassie-stained SDS−PAGE.

Purification of eNOS. Bovine pulmonary arterial endothelial NOS (eNOS) was prepared and characterized as described previously (*37*). These preparations of endothelial NOS routinely possessed a specific activity of 0.15 μmol of citrulline formed min^{-1} (mg of protein)$^{-1}$ when assayed at saturating arginine concentrations.

NO Formation Assay. Nitric oxide production over time was measured spectrophotometrically at 401 nm by the conversion of oxyhemoglobin to methemoglobin (*38*). Reaction mixtures contained 50 mM Hepes, pH 7.5, 100 μM NADPH, 0.003 mg/mL calmodulin, 1 mM EGTA, 2 mM Ca^{2+}, 100 μM L-arginine, 5 μM oxyhemoglobin, and 0.15 μM BH_4 and were initiated by the addition of nNOS sample. Methemoglobin formation was monitored against a reference cuvette containing complete reaction mixture without enzyme. NO production was calculated using an extinction coefficient of 38 mM^{-1} cm^{-1} (*38*).

Citrulline Formation Assay. Citrulline formation by NOS isoforms was measured in 150 μL reaction mixtures containing 30 mM Hepes, pH 7.5, 1 mM DTT, 120 nM L-[2,3-^{3}H]-arginine without or with unlabeled arginine as indicated in the appropriate legends, 1 mM EGTA, 0.85 mM Ca^{2+} (when present), 6 μM CaM (when present), 100 μM NADPH, and 300 μM BH_4. Incubations were initiated by the addition of enzyme, reaction mixtures incubated for 30 min at 30 °C in duplicate, and reactions stopped and analyzed as described by Wolff and Datto (*8*).

Assay of NADPH-Oxidase Activity. Standard reaction mixtures of 1 mL volume in quartz cuvettes contained 50 mM Hepes, pH 7.4, 150 μM NADPH, 6 μM CaM, 1 mM EGTA, 0.85 mM Ca^{2+}, and 0.15 μM BH_4. Reactions were initiated by the addition of nNOS enzyme, and NADPH consumption was measured from the change in light absorbance at 340 nm as compared to an identical reference cuvette without enzyme using an extinction coefficient of 6.22 mM^{-1} cm^{-1}.

Cytochrome c Reductase Assay. The cytochrome *c* reductase activity of nNOS was determined as described previously (*39*) in the presence of 1 mM EGTA, 2 mM Ca^{2+}, and 10 μg/mL CaM. An extinction coefficient of 21 mM^{-1} cm^{-1} was used to quantify cytochrome *c* reduction.

Determination of Hydrogen Peroxide. Hydrogen peroxide was determined by the formation of ferric thiocyanate as described by Heinzel et al. (*40*). NO synthase was incubated at 30 °C for 20 min in 500 μL of 50 mM Hepes, pH 7.4, 0.5 mM DTT, 200 μM NADPH, 1 mM EGTA, 2 mM Ca^{2+}, and 2 μM CaM. Reactions were terminated by the addition of 300 μL of HCl (12 M). The color was developed by addition of 60 μL of ferrous ammonium sulfate (50 mM) and 90 μL of sodium thiocyanate (2 M). Samples were incubated for 10 min at ambient temperature followed by the immediate determination of light absorbance at 492 nm. Blank values were determined in the presence of enzyme but with 20 μg of catalase present. These values were identical to values stopped at zero time. Values were determined by comparison to a standard curve containing 0.25−25 μM hydrogen peroxide.

Miscellaneous. Protein concentrations were determined by the method of Bradford (*41*) with bovine serum albumin as the standard.

RESULTS

Isoform Selectivity of NOS Inhibition by Fullerene Monomalonate Adducts. In an initial experiment to determine the

Table 1: Determination of the IC_{50} Values for Diverse Monofullerene Adducts versus the Three Nitric Oxide Synthase Isoforms[a]

compound	inducible NOS (μM)	neuronal NOS (μM)	endothelial NOS (μM)
diamine adduct	19	2.5	77
diol adduct	110	4.0	220
semi-amine adduct	85	11	89

[a] Standard incubations were constructed for measurement of citrulline formation in incubations containing 120 nM arginine as described under Experimental Procedures in the absence and presence of concentrations of fullerene adducts ranging from 0.3 to 300 μM. The concentration of agent providing 50% inhibition of activity in a 30 min incubation is indicated above. Incubations were initiated with an enzyme dilution that provided less than 10% consumption of arginine substrate as measured in the absence of added agent.

potency and isoform selectivity of fullerene monomalonate adducts, we examined their effect on the citrulline formation rate catalyzed by each of the NOS isoforms in incubations conducted for a fixed period of time (Table 1). Each of the adducts was found to exhibit their greatest potency versus the neuronal as compared to either the endothelial or the cytokine-inducible isoform, with the diamine adduct being slightly more potent than the diol adduct. Of the fullerenes tested, the diol adduct exhibited the greatest isoform selectivity, inhibiting the neuronal isoform at concentrations 55-fold lower than those required to inhibit the endothelial isoform and 28-fold lower than those required to inhibit the cytokine-inducible isoform. Considering their potency and selectivity versus the neuronal NOS, subsequent experiments focused on the mechanism of their inhibition of this isoform.

Effect of the Diol Adduct on the Catalytic Competencies of nNOS. Many inhibitors of nitric oxide synthase isoforms have been described that fall into two major mechanistic classes. Some inhibitors bind rapidly and reversibly, resulting in an enzymatic activity that produces NO and citrulline at a reduced but linear rate. Other inhibitors either are irreversible, slow-binding, slowly dissociating or are turnover-based suicide inhibitors that suppress enzymatic activity such as to produce NO and citrulline at a rate that progressively diminishes over time. To explore the behavior of the diol adduct with respect to the time dependence of its inhibition of NOS activity, we examined its inhibition of NO formation using a continuous, real time assay measuring its effect spectrophotometrically on methemoglobin formation (Figure 2). As measured in the presence of 20 μM diol adduct, nNOS catalyzed NO production at a rate that rapidly decreased to an undetectable rate over an 8 min period. This phenomenon may be attributable to several causes that include the following. It is possible that the fullerene is a high-affinity but slow-binding inhibitor or, alternately, the fullerene may promote the formation of an alternate, inhibitory product that accumulates in solution. Given the known structure of the diol adduct which does not resemble that of arginine substrate, we thought it unlikely that it served as an alternate substrate or that it covalently derivatized the enzyme directly. To provide a clearer understanding of its behavior, we examined the effect of adding a second increment of nNOS enzyme following the apparent complete inactivation of the first nNOS increment (Figure 2, panel A). When a second nNOS increment was added after 10 min, NO formation resumed only briefly, with complete inactivation occurring

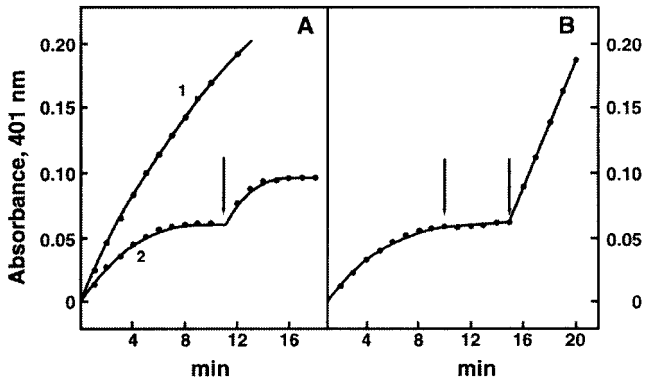

FIGURE 2: C_{60}-Diol adduct produces a time-dependent suppression of nNOS activity altered by superoxide dismutase−catalase. (A) Standard incubations were constructed in 1 mL polystyrene cuvettes containing 50 mM Hepes, pH 7.4, 100 μM arginine, 0.15 μM BH_4, 150 μM NADPH, 5 μM oxyhemoglobin, 6 μM CaM, 1 mM EGTA, 1.5 mM Ca^{2+} without (curve 1) or containing 20 μM (curve 2) diol adduct. Reactions were initiated at zero time with 8 μg of GH_3 pituitary nNOS. At 11 min post-initiation, a second 8 μg portion of nNOS was added to the fullerene-containing incubation. NO formation throughout was measured as the NO-dependent formation of methemoglobin measured spectrophotometrically. (B) Conditions are identical to those described for curve 2, panel A; however, at 10 min post-initiation, 10 μg of superoxide dimutase and 10 μg of catalase were added for 5 min, prior to the addition at 15 min of a second 8 μg nNOS sample.

after a period of only 4 min, as compared to the 8 min required to inactivate the first increment of nNOS. This suggested the possibility that during the initial 10 min a product had accumulated in solution that acting from solution produced a time-dependent inactivation of activity. The neuronal NOS isoform has been reported by many laboratories (*40*, *42*−*48*) to produce reactive oxygen intermediates including superoxide anion free radical and hydrogen peroxide that dissociate from the enzyme accompanied by a slow rate of autoinactivation. This phenomenon, however, is normally almost completely suppressed in the presence of high concentrations of arginine substrate and tetrahydrobiopterin cofactor. We considered the possibility that in the presence of fullerene the dissociation of reactive oxygen intermediates might be enhanced despite the presence of arginine and tetrahydrobiopterin. Accordingly, we repeated the experiment (Figure 2, panel B) adding, after 10 min, a mixture of superoxide dismutase (SOD) and catalase in order to destroy any potential reactive oxygen intermediates that may have accumulated in solution during the first 10 min of turnover. Now, at 5 min after the addition of superoxide dismutase and catalase, a second nNOS addition was made. A markedly increased rate of NO formation occurred following this addition that corresponded closely to the rate observed when SOD and catalase were present from time zero (see Figure 3, panel B). These observations are consistent with the proposal that the time-dependent loss of activity seen in the presence of fullerene was due to the accumulation of superoxide anion and/or hydrogen peroxide produced by the enzyme that, acting from solution, were responsible for the time-dependent activity loss. These accumulating, inactivating substances were presumably removed during the 5 min exposure to SOD and catalase, and prevented their accumulation following the addition of the second nNOS increment, resulting in the now rapid and apparently uninhibited rate of NO formation.

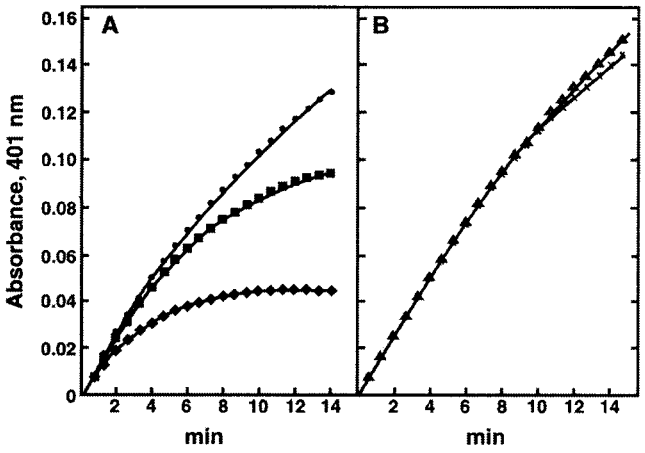

FIGURE 3: Effect of the C_{60}-diol adduct on time-dependent NO formation by GH_3 pituitary nNOS in the absence and presence of superoxide dismutase and catalase. Panel A: Methemoglobin formed from the reaction of oxyhemoglobin with NO was measured in standard incubations containing 100 μM arginine in disposable cuvettes as described under Experimental Procedures without (●) or with 10 (■) or 20 (◆) μM diol adduct. Panel B: Effect of the addition of superoxide dismutase and catalase. Measurements of methemoglobin formation were conducted in incubations identical to those of panel A but contained 10 μg of superoxide dismutase and 10 μg of catalase without (△) or containing (×) 20 μM diol adduct.

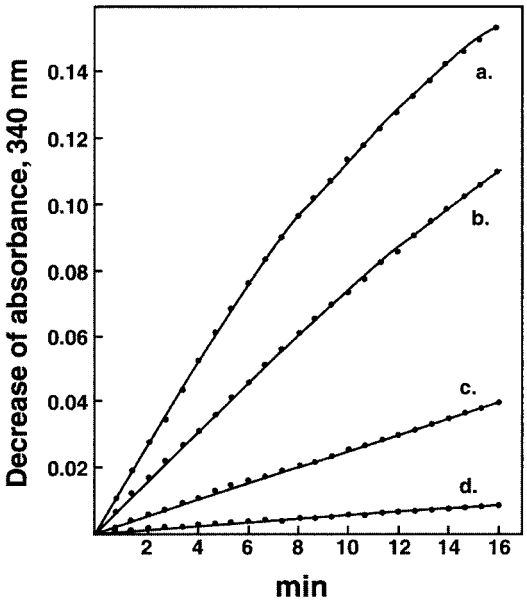

FIGURE 4: Effect of the diol adduct on Ca^{2+}-dependent NADPH consumption by GH_3 pituitary nNOS. Standard reactions of 1 mL volume were constructed in quartz cuvettes containing 50 mM Hepes, pH 7.4, 0.6 μM CaM, 1 mM EGTA, 150 μM NADPH, 2 mM Ca^{2+}, 0.15 μM BH_4, and 12 μg of nNOS. Incubations contained (curve a) no further additions; (curve b) 20 μM diol adduct and 100 μM arginine; (curve c) 100 μM arginine; or (curve d) 100 μM arginine, 20 μM diol adduct, 1 mM glucose, 20 μg of glucose oxidase, 10 μg of catalase.

To confirm this further, we examined the nNOS-catalyzed time-dependent formation of NO in incubations without or containing 10 or 20 μM diol adduct in the absence of SOD−catalase (Figure 3, panel A) or in the presence from time zero of SOD−catalase (Figure 3, panel B). As measured without either fullerene or SOD and catalase, a slow, time-dependent loss of NO-forming activity was observed. This is consistent with the widely described (*33*, *40*, *41*) slow, autoinactivation rate of the nNOS isoform. As measured in the absence of SOD and catalase, this rate of inactivation was clearly enhanced by the presence of either 10 or 20 μM diol adduct. As measured in the presence of SOD and catalase, the inhibitory effect of fullerene was virtually completely eliminated. When SOD and catalase were tested separately, a partial but incomplete protection was afforded.

Using identical protocols, the effect of diol adduct was measured on the time-dependent formation of NO catalyzed by either iNOS or eNOS (data not shown). For these isoforms, higher concentrations of fullerene adduct were needed to produce significant inhibition of product formation. However, in the presence of these inhibitory concentrations of fullerene, depressed but linear rates of product formation were observed. Hence, inhibition of these isoforms did not progress with time and were fully reversible, and therefore presumably were the result of a different mechanism of inhibition.

As measured in the absence of arginine, nNOS catalyzes the formation of superoxide anion and hydrogen peroxide by reducing oxygen bound to the heme iron residue using reducing equivalents derived from NADPH, an activity commonly referred to as its substrate-independent NADPH-oxidase activity (*40*, *46*). Upon addition of arginine, the production of dissociating reactive oxygen intermediates is suppressed as their formation is now linked to the two-step oxidation of arginine to *N*-hydroxyarginine and subsequently to citrulline and nitric oxide formation (*40*, *46*). Under these conditions, the accumulating NO binds to the heme iron, leading to the inhibition of nNOS activity (*44*, *49*). This leads to a decreased rate of NADPH consumption accompanying the formation of NO and citrulline. We measured the effect of the diol adduct on the NADPH consumption rate of nNOS in the absence and presence of arginine substrate (Figure 4). As measured in the absence of either arginine or fullerene, a rapid rate of NADPH consumption was observed (curve a). At this condition, NADPH consumption is known to be linked to the reduction of oxygen. When these measurements were repeated in the absence of arginine but in the presence of 20 μM diol adduct, an identical rate of NADPH consumption was observed (not shown). As measured in the presence of arginine but absence of fullerene (curve c), a markedly suppressed (85% reduction) NADPH consumption rate was observed as compared to the identical condition without arginine. However, when both arginine and 20 μM diol adduct were present (curve b), a markedly enhanced NADPH consumption rate was observed (despite the presence of arginine) that achieved a rate 73% of the rate observed in the absence of arginine (curve a). Presumably this increased NADPH consumption rate is linked entirely to the reduction of oxygen and the generation of superoxide anion and hydrogen peroxide. To test this presumption, we repeated the measurement of NADPH consumption in the presence of both arginine and fullerene but now added glucose, glucose oxidase, and catalase (curve d). Glucose, glucose oxidase, and catalase lead to the rapid depletion of oxygen, consuming it in the production of gluconic acid. This procedure has been widely used to dramatically reduce oxygen levels (*4*, *51*). At this condition (curve d), the NADPH consumption rate was reduced to near zero, consistent with the proposal that the increased NADPH consumption observed in the concurrent presence of arginine

and fullerene was linked to the reduction of oxygen. As measured in the presence of fullerene but without added nNOS, no NADPH consumption was measurable, indicating that the increased oxygen reduction was nNOS-catalyzed (not shown).

Two pathways for the increased reduction of oxygen in the concurrent presence of arginine and fullerene can be envisioned. In the first pathway, electron transfer within nNOS follows the normal route in which reactive oxygen intermediates bound to the heme iron are formed, that in the presence of fullerene dissociate into solution rather than attacking the guanidino nitrogen of arginine. The second pathway would resemble that observed for adriamycin (*52*) in which adriamycin accepts electrons from a reductase domain flavin to form the hydroquinone form of this drug which subsequently donates its electron to oxygen, leading to the formation of superoxide anion. Nitroarginine is known to reduce to near zero the NADPH consumption rate of nNOS, but does not prevent the unrestricted flow of electrons through its reductase domain as revealed by its failure to inhibit the cytochrome *c* reductase activity of nNOS. This action has been attributed to the ability of nitroarginine to alter the reduction potential of the heme iron such that oxygen binding does not occur (*40, 53*). These considerations predict that if the first pathway is followed, nitroarginine would completely inhibit NADPH consumption in the presence of fullerene, while if pathway 2 is followed no inhibition would be expected. When the experiment was run (not shown), nitroarginine completely inhibited NADPH consumption in the presence of fullerene.

A further experiment indicating that fullerenes do not "steal" electrons from the reductase domain was provided by examining the effects of the diol adduct on the cytochrome *c* reductase activity of nNOS. The effect of fullerene on the cytochrome *c* reductase activity of nNOS was measured at concentrations of fullerene up to 50 μM. The diol adduct had no effect on activity and maintained unaltered activity despite conditions supporting enzyme turnover for periods up to 15 min (not shown). At these conditions, the NO formation rate is dramatically reduced (Figures 2 and 3) by the diol adduct.

Reversibility of the Effect of Diol Adduct and Its Dependence on Turnover. To examine whether the effects of the diol adduct on nNOS activity are reversible, we employed a preincubation paradigm (Figure 5). Samples of nNOS were preincubated in the absence and presence of fullerene in the absence and concurrent presence of superoxide dismutase−catalase. Initially the preincubations did not contain Ca^{2+}, and therefore the nNOS was exposed to fullerene under conditions that would not support catalytic turnover. Samples withdrawn from the incubations at these conditions showed no loss of activity over time. The preincubations were adjusted at 12 min to contain Ca^{2+}, thus converting nNOS to its catalytically active form. As measured in the absence of fullerene, SOD, and catalase, 60% of the initial activity was retained 21 min following Ca^{2+} addition. The presence of SOD−catalase provided no protection against this inactivation. Preincubations containing fullerene but without SOD−catalase lost activity at a markedly higher rate, with only 13% of the initial activity remaining after 21 min of exposure. When SOD−catalase was added to the fullerene preincubation, the fullerene-dependent increased rate of inactivation was completely reversed to the rate obtained in the absence of fullerene. In an experiment not shown, either SOD alone or catalase alone provided partial protection, but not full protection. Since samples from the preincubation are diluted 50-fold for the assay of residual activity, the fullerene delivered from the preincubation into the assay is diluted from a concentration known to be inhibitory in an assay to a value known to be noninhibitory. Thus, it is clear that the effects of fullerene on activity are irreversible and require catalytic turnover to produce their inactivation.

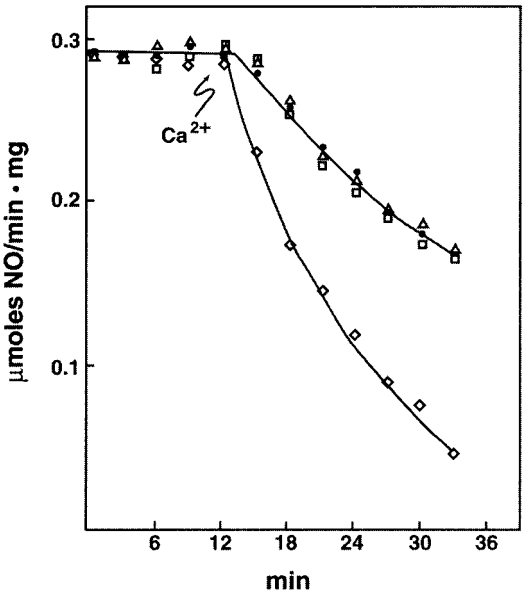

FIGURE 5: Effect of diol adduct on Ca^{2+}-dependent inactivation of GH_3 pituitary nNOS. Preincubations were constructed of 700 μL final volume containing 50 mM Mops, pH 7.4, 1 mM DTT, 1 mM arginine, 0.1 μM CaM, 2.5 mM NADPH, 225 μg of nNOS. Preincubations were initiated by the addition of nNOS and were conducted at 25 °C. Samples (50 μL) were removed at zero time and at subsequent 3 min intervals were used to initiate standard NO formation (measured as methemoglobin) assays that were conducted for 2 min to measure residual nNOS activity in the preincubated samples. At 12 min post-initiation, the nNOS in each preincubation was converted to its catalytically active form by adjustment of total [Ca^{2+}] to 1 mM. Preincubations were conducted at 4 conditions: (●) no further additions; (◇) containing 20 μM diol adduct; (△) containing 10 μg of superoxide dismutase, 10 μg of catalase; (□) containing 20 μM diol adduct, SOD, and catalase.

Effect of the Diol Adduct on the Kinetic Behavior of nNOS. To clarify whether the effect of fullerene is mediated by a competitive displacement of arginine from nNOS, we examined the arginine concentration dependence of citrulline formation in the absence and presence of 1.5, 5, or 15 μM diol adduct (Figure 6). The fullerene reduced the maximal velocity of citrulline formation but did not alter the apparent K_m for arginine substrate. Similarly we measured the effect of fullerene on the tetrahydrobiopterin concentration dependence of citrulline formation (Figure 7). Since the tetrahydrobiopterin cofactor is a known reducing agent that provides enzyme stabilization to autoinactivation (*47, 54*), we were interested in whether BH_4 provided protection against fullerene-induced inactivation. Accordingly the BH_4 concentration dependence of nNOS activity was measured in incubations without or containing either 1.5 or 5 μM fullerene. The presence of fullerene reduced the maximal velocity of citrulline formation but did not alter the EC_{50} value for BH_4 stimulation of activity. Thus, the inhibition

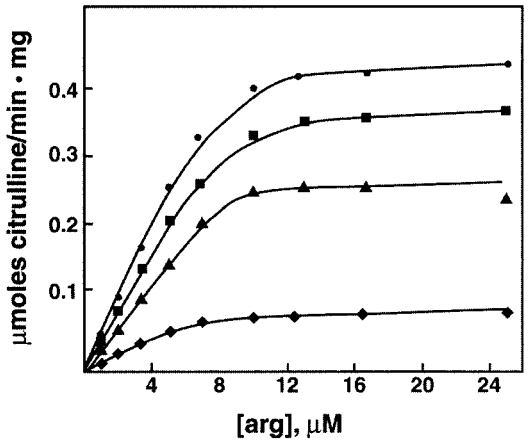

FIGURE 6: Effect of the diol adduct on the arginine concentration dependence of GH_3 pituitary nNOS. Standard incubations were constructed without (●) or containing 1.5 (■), 5 (▲), or 15 (◆) μM diol adduct and the indicated concentrations of arginine. Incubations were initiated with 0.8 μg of GH_3 pituitary nNOS. Data are plotted as the μmol of citrulline formed min^{-1} mg^{-1} at the specified arginine concentration.

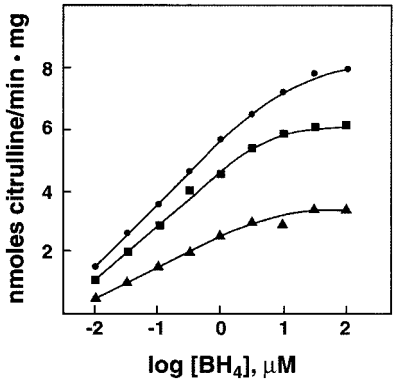

FIGURE 7: Effect of the diol adduct on the tetrahydrobiopterin concentration dependence of GH_3 pituitary nNOS. Standard incubations containing 120 nM arginine were constructed without (●) or containing 1.5 (■) or 5 (▲) μM diol adduct and the indicated concentrations of BH_4. Incubations were initiated with 0.09 μg of GH_3 nNOS. Values are expressed as the nmol of citrulline formed min^{-1} (mg of protein)$^{-1}$. BH_4 concentrations are plotted on a log scale to permit presentation over a 10 000-fold range of values.

of citrulline formation was not surmountable by an increased concentration of BH_4.

We examined the effect of the monoalcohol fullerene adduct on the calmodulin (CaM) dependence of citrulline formation (Figure 8). Citrulline formation was measured in incubations without or containing 1.5, 5, or 15 μM fullerene. The presence of fullerene reduced the maximal velocity of citrulline formation but did not alter the EC_{50} value for CaM. Clearly the effect of fullerene was not surmountable by increased concentrations of CaM.

Effect of Fullerene on Hydrogen Peroxide Production by nNOS. The experiments described above indicate that the diol adduct under normal assay conditions produces a time-, concentration-, and turnover-dependent inactivation of the catalytic competence of nNOS to form nitric oxide. This inactivation is fully prevented by enzymes that catalyze the destruction of superoxide anion free radical and hydrogen peroxide. These observations strongly suggest that the presence of fullerenes uncouples the production of reactive oxygen intermediates from NO production. Accordingly we

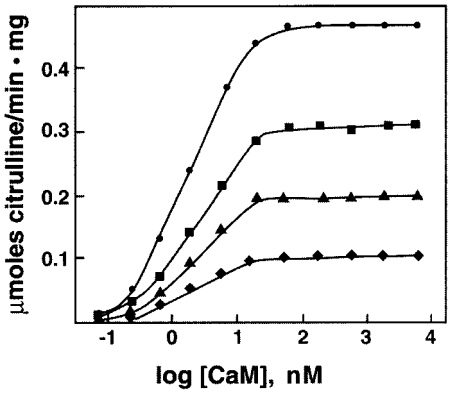

FIGURE 8: Effect of the diol adduct on the CaM dependence of GH_3 pituitary nNOS. Standard incubations for measurement of citrulline formation by nNOS were constructed without (●), or containing 1.5 (■), 5 (▲), or 15 (◆) μM diol adduct and the indicated concentrations of CaM. Incubations were initiated with 0.5 μg of nNOS and were conducted for 30 min. Values are expressed as the μmol of citrulline formed min^{-1} (mg of protein)$^{-1}$. Calmodulin concentration values are plotted on a log scale to permit presentation over a 100 000-fold variation of values.

Table 2: Effect of the Diol and Diamine Adducts on Hydrogen Peroxide Formation by nNOS[a]

additives	H_2O_2 formation rate (nmol min^{-1} mg^{-1})
none	301 ± 8
arginine	5 ± 3
diol adduct, 30 μM	293 ± 6
arginine + diol adduct	142 ± 5
diamine adduct, 30 μM	291 ± 7
arginine + diamine adduct	286 ± 7

[a] Incubations of 600 μL volume were constructed containing 50 mM Hepes, pH 7.4, 0.5 mM DTT, 150 μM NADPH, 0.5 μM BH_4, 0.5 mM EGTA, 1 mM Ca^{2+}, 0.3 μM CaM, without or containing 400 μM arginine, without or containing fullerene adduct as indicated. Incubations were initiated with 24 μg of nNOS and were incubated at 30 °C for 20 min. A 500 μL portion was removed for analysis of hydrogen peroxide production performed as described under Experimental Procedures. A paired incubation identical in all respects but containing 20 μg of catalase was used as a control, and their values ($A_{492\ nm}$) were subtracted from the paired incubation without catalase to determine the specific hydrogen peroxide contribution to absorbance. Values are expressed as nmol of hydrogen peroxide formed min^{-1} (mg of protein)$^{-1}$ by comparison to values obtained from a hydrogen peroxide standard curve.

measured directly the effect of fullerenes on hydrogen peroxide production by nNOS in the presence and absence of arginine (Table 2). As measured in the absence of fullerene, arginine as reported previously (*40*) produced an almost complete suppression of hydrogen peroxide production. As measured in the absence of arginine, the diol adduct had no effect on hydrogen peroxide production. However, as measured in the concurrent presence of arginine and fullerene, a dramatic increase of hydrogen peroxide production was observed, achieving a value almost 50% of that observed in the absence of arginine. The diamine adduct behaved similarly, producing hydrogen peroxide at a rate comparable to that seen in the absence of arginine despite the presence of arginine. The monoamine fullerene adduct behaved qualitatively similarly (data not shown).

DISCUSSION

A series of monosubstituted C_{60}-fullerene adducts have been examined for effects on the activities of the three nitric

oxide synthase isoforms. These adducts inhibited citrulline formation by all three isoforms but, in fixed time incubations, clearly demonstrated a greater inhibitory potency versus the neuronal NOS isoform. The inhibition of nNOS-catalyzed NO formation by these adducts increased progressively over time, while the inhibition of NO formation by either the inducible or the endothelial isoforms required much higher concentrations of adduct and led to NO production at reduced but linear rates. These observations are consistent with a reversible mechanism of activity suppression of fullerene monomalonate adducts versus the iNOS and eNOS isoforms while exhibiting an apparently irreversible mechanism versus the nNOS isoform.

Since the diol adduct exhibited the greatest isoform selectivity in inhibiting the NOS isoforms, we have characterized its behavior extensively. The diol C_{60}-fullerene adduct produced a time-, concentration-, and turnover-dependent inactivation of neuronal NOS NO-forming activity. This adduct promoted the consumption of NADPH as measured in the presence of arginine but had no effect in its absence. This increased consumption of NADPH was linked to oxygen as the terminal electron acceptor as evidenced by the virtually complete suppression of the fullerene-enhanced NADPH consumption by nitroarginine or by the concurrent presence of glucose, glucose oxidase, and catalase that creates a state of profound oxygen depletion. In the concurrent presence of diol adduct and arginine, we observed a dramatic increase in the production of hydrogen peroxide (Table 2) as well as a decrease in the NO production rate that progressed over time (Figures 2 and 3). This decreased NO production rate could be prevented by the concurrent presence of superoxide dismutase and catalase. Since the SOD and catalase can destroy only reactive oxygen intermediates that have dissociated from nNOS into solution, this indicates that the inactivation produced by these reactive oxygen intermediates does not occur at the catalytic site prior to dissociation, but that they inactivate from solution following dissociation.

Since the fullerene monomalonate adducts do not resemble structurally any of the known substrates or cofactors of NOS and indeed interact qualitatively differently with nNOS than with the other NOS isoforms, it is not clear a priori where the interaction site of fullerene monomalonate adducts is to be found on nNOS. The adducts do not appear to interact with the reductase domain since they had no effect on the cytochrome *c* reductase activity of this isoform even when measured at conditions at or below the K_m of nNOS for cytochrome *c*. Thus, the fullerene monomalonate adducts do not appear to be alternate electron acceptors that "steal" electrons from the reductase domain, since such an activity would inhibit the reduction of cytochrome *c*. Some fullerenes in the presence of light are able to interact with oxygen to generate superoxide anion (*19, 20, 54*). The effects observed here are not light-dependent since no inactivation by fullerenes was observed in the presence of ambient light, unless and until nNOS was converted to its catalytically active form by the presence of Ca^{2+} and CaM (Figure 5). These studies indicated clearly that the fullerene-mediated inactivation of nNOS required turnover but not light. Further, there is no apparent reason a light-dependent mechanism of inactivation should apply only to the nNOS but not the iNOS or eNOS isoform. Some agents, such as adriamycin, are able to accept electrons from the reductase domain of NOS, with their reduced hydroquinone form subsequently interacting with oxygen to produce superoxide anion radical. This mechanism is apparently also not operative here, since nitroarginine, which has no effect on electron transfer within the reductase domain, but does inhibit the reduction of heme iron, and subsequently the reduction of oxygen at the heme-containing catalytic domain, inhibits the fullerene-enhanced consumption of NADPH. This is consistent with the proposal that the enhanced NADPH consumption linked to oxygen reduction requires the binding of oxygen to its reduced heme iron binding site on nNOS.

The fullerene monomalonate adducts do not exert their effects on NOS by altering its interaction with CaM since their inhibitory effects could not be overcome at dramatically increased concentrations of CaM. Further, the concentration of CaM required to activate nNOS activity was unaltered in the presence of these fullerenes.

Finally, the fullerene monomalonate adducts, while altering the behavior of the catalytic domain of nNOS, do not appear to occupy it since they altered neither the arginine nor the tetrahydrobiopterin concentration dependence of activity and exerted effects insurmountable by markedly elevated concentrations of these ligands which are known to occupy the catalytic site of NOS. Other inhibitors such as the imidazoles and indazoles (*37, 55*−*57*) that occupy the catalytic site are known to exert inhibitions that are competitive versus arginine and BH_4, since their large size occupies space that disallows the concurrent binding of these inhibitors and either arginine or BH_4. The inhibition of citrulline formation by the fullerene monomalonate adducts, however, was not competitive with these ligands and was insurmountable by them. Given that the dimensions of the fullerenes are larger than either the imidazole or the indazoles, the observation of their noncompetitive inhibition of nNOS is inconsistent with the occupancy by the fullerene monomalonate adducts of the nNOS catalytic site.

Our laboratory has previously reported the inhibition of NOS isoforms by the C_3 and D_3 **tris**malonic C_{60} derivatives (*29*). This inhibition was clearly different in character than the one reported here for the fullerene **mono**malonate adducts. Trismalonic fullerenes produced an inhibition of NOS isoforms that was not isoform-selective and was fully reversible. The trismalonic fullerenes inhibited almost completely the reduction of nNOS-catalyzed NADPH consumption as measured in the absence of arginine, an activity that indicated that they block the intersubunit transfer of electrons necessary to support the substrate-independent NADPH-oxidase activity of nNOS. The monoderivatized fullerenes by contrast produce a selective, irreversible inactivation of the nNOS isoform and have no effect on the substrate-independent NADPH-oxidase activity of nNOS. The fullerene monomalonate adducts each possess a virtually unblemished, spherical, hydrophobic domain (see Figure 1) that presumably is necessary for it to exert its destabilizing effect on the nNOS isoform. The triply derivatized fullerenes possess hydrophobic domains of more limited dimension, being shielded at several sites by the multiple attachment of highly ionized, hydrophilic structures.

In conclusion, we report here that fullerene monomalonate adducts interact with nNOS to so distort its structure as to dissociate the formation of reactive oxygen intermediates from their subsequent successful coupling to the oxidation

of arginine to elicit NO and citrulline formation. The dissociated oxygen intermediates including superoxide anion and hydrogen peroxide, acting from solution, inactivate nNOS. Such behavior provides a unique mechanism for the isoform-selective inhibition of nNOS.

REFERENCES

1. Nathan, C. A. (1992) *FASEB J. 6*, 3051−3064.
2. Bredt, D. S,. and Snyder, S. H. (1992) *Neuron 8*, 3−11.
3. Rees, D. D., Palmer, R. M. J., and Moncada, S. (1989) *Proc. Natl. Acad. Sci. U.S.A. 86*, 3375−3378.
4. MacMicking, J. D., Xie, Q.-W., and Nathan, C. (1997) *Annu. Rev. Immunol. 15*, 323−350.
5. Griffith, O. W., and Stuehr, D. J. (1995) *Annu. Rev. Physiol. 57*, 707−736.
6. Bryk, R., and Wolff, D. J. (1999) *Pharmacol. Ther. 84*, 157−178.
7. Forstermann, U., Gath, I., Schwarz, P., Closs, E. I., and Kleinert, H. (1995) *Biochem. Pharmacol. 9*, 1321−1332.
8. Wolff, D. J., and Datto, G. (1992) *Biochem. J. 284*, 201−206.
9. Stuehr, D. J., Cho, H. J., Kwon, N. S., Weise, M. F., and Nathan, C. A. (1991) *Proc. Natl. Acad. Sci. U.S.A. 88*, 7773−7777.
10. Hevel, J. M., White, K. A., and Marletta, M. A. (1991) *J. Biol. Chem. 266*, 22789−22791.
11. Lamas, S., Marsden, P. A., Li, G. K., Tempst, P., and Michel, T. (1992) *Proc. Natl. Acad. Sci. U.S.A. 87*, 3629−3632.
12. Kilbourn, R. G., Gross, S. S., Jubran, A., Adams, J., Griffith, O. W., Levi, R., and Lodato, R. F. (1990) *Proc. Natl. Acad. Sci. U.S.A. 87*, 3629−3632.
13. Hooper, D. C., Bagasra, O., Marini, J. C., Zborek, A., Ohnishi, S. T., Kean, R., Champion, J. M., Sarker, A. B., Bobroski, L., Fraber, J. L., Takaaki, A., Hiroshi, M., and Kaprowski, H. (1997) *Proc. Natl. Acad. Sci. U.S.A. 94*, 2528−2533.
14. McCartney-Francis, N., Allen, J. B., Mizel, D. E., Albina, J. E., Xie, Q.-W., Nathan, C., and Wahl, S. M. (1993) *J. Exp. Med. 178*, 749−754.
15. Huang, Z., Huang, P., Panahian, N., Dalkara, T., Fishman, M. C., and Moskowitz, M. A. (1990) *Science 265*, 1883−1888.
16. Hantraye, P., Brouillet, E., Ferrante, R., Palfi, S., Dolan, R., Matthews, R. T., and Beal, M. F. (1996) *Nat. Med. 2*, 1017−1021.
17. Kroto, H. W., Heath, J. R., O'Brien, S. C., Curl, R. F., and Smalley, R. E. (1985) *Nature 318*, 162−163.
18. Kratschner, W., Lamb, L. D., Fostiropoulos, K., and Huffman, D. R. (1990) *Nature 347*, 354−358.
19. Jensen, A. W., Wilson, S. R., and Schuster, D. I. (1996) *Bioorg. Med. Chem. 4*, 767−777.
20. DaRos, T., and Prato, M. (1999) *Chem Commun.*, 663−669.
21. Richardson, C. F., Schuster, D. I., and Wilson, S. R. (2000) *Org. Lett. 2*, 1011−1014.
22. Ruoff, R. S., Tse, D. S., Malhotra, R., and Lorents, D. C. (1993) *J. Phys. Chem. 97*, 3379−3386.
23. Tokuyama, H., Yamaga, S., Nakamura, E., Shiraki, T., and DSuguira, Y. (1993) *J. Am. Chem. Soc. 115*, 7918−7923.
24. Friedman, S. H., Decamp, D. L., Sijbesma, R. P., Srdanov, G., Wudl, F. and Kenyon, G. L. (1993) *J. Am. Chem. Soc. 115*, 6506−6509.
25. Schinazi, R. F., Sijbesma, Svadanov, G., Hill, C. L., and Wudl, F. (1993) *Antimicrob. Agents Chemother. 37*, 1707−1710.
26. Wilson, S. R. (2000) Biological Aspects of Fullerenes. in *Fullerenes: Chemistry, Physics and Technology* (Kadish, K. M., and Ruoff, R. S., Eds.) pp 431−436, John Wiley and Sons, New York.
27. Dugan, L. L., Turetsky, D. M., Du, C., Lobner, D., Wheeler, M., Almli, C. R., Shen, C. K.-F., Luh, T. Y., Choi, D. W., and Lin, T. S. (1997) *Proc. Natl. Acad. Sci. U.S.A. 94*, 9434−9439.
28. Dugan, L. L., Lovett, E., Cuddihy, Ma, B., Lin, T., and Choi, D. Carboxyfullerenes as Neuroprotective Antioxidants. in *Fullerenes: Chemistry, Physics and Technology* (Kadish, K. M., and Ruoff, R. S., Eds.) pp 467−479, John Wiley and Sons, New York.
29. Wolff, D. J., Papoiu, A. D. P., Mialkowski, K., Richardson, C. F., Schuster, D. I., and Wilson, S. R. (2000) *Arch. Biochem. Biophys. 378*, 216−223.
30. Cooper, G. R., Barr, A., and Wolff, D. J. (1998) *Arch. Biochem. Biophys. 357*, 195−206.
31. Camps, X., and Hirsch, A. (1997) *J. Am. Chem. Soc., Perkins Trans I*, 1595−1596.
32. Schuster, D. I., Cao, J., Kaprinidis, N., Wu, Y., Jensen, A. W., Lu, Q., Wang, H., and Wilson, S. R. (1996) *J. Am. Chem. Soc. 118*, 5639−5647.
33. Cross, R. J., Jiminez-Vasquez, H. A., Lu, Q., Saunders, M., Schuster, D. I., Wilson, S. R., and Zhao, H. (1996) *J. Am. Chem. Soc. 118*, 114454−11459.
34. Jensen, A. W., Khong, A., Saunders, M., Wilson, S. R., and Schuster, D. I. (1997) *J. Am. Chem. Soc. 119*, 7303−7307.
35. Ruttiman, M., Haldimann, L. R. F., Isaacs, L., Diederich, F., Khong, A., Jiminez-Vasquez, H. A., Cross, R. J., and Saunders, M. (1997) *Chem. Eur. J. 3*, 1071−1076.
36. Bryk, R., and Wolff, R. (1998) *Biochemistry 37*, 4844−4852.
37. Wolff, D. J., Lubeskie, A., and Umansky, S. (1994) *Arch. Biochem. Biophys. 312*, 360−366.
38. Noack, E., Kubitzak, D., and Kodja, I. (1992) *Neuroprotocols 1*, 133−139.
39. Cooper, G. R., Mialkowsi, K., and Wolff, D. J. (2000) *Arch. Biochem. Biophys. 375*, 183−194.
40. Heinzel, B., John, M., Klatt, P., Bohma, E., and Mayer, B. (1992) *Biochem. J. 281*, 627−630.
41. Bradford, M. M. (1976) *Anal. Biochem. 72*, 248−254.
42. Kotsonis, P., Frey, A., Frohlich, L. G., Hofmann, H., Reif, A., Wink, D. A., Feelisch, M., and Schmidt, H. H. W. (1999) *Biochem. J. 340*, 745−752.
43. Pou, S., Pou, W. S., Bredt, D. S., Snyder, S. H., and Rosen, G. M. (1992) *J. Biol. Chem. 267*, 24173−24176.
44. Wolff, D. J., and Lubeskie, A. (1995) *Arch. Biochem. Biophys. 316*, 290−301.
45. Vasquez-Vivar, J., Hogg, N., Martasek, P., Karoui, H., Pritvhard, K. A., and Kalyanaraman, B. (1999) *J. Biol. Chem. 274*, 26736−26742.
46. Klatt, P., Schmidt, K., Uray, G., and Mayer, B. (1993) *J. Biol. Chem. 268*, 14781−14787.
47. Kotsonis, P., Frohlich, L. G., Shutenko, Z. V., Horejsi, R., Pfleiderer, W., and Schmidt, H. H. W. (2000) *Biochem. J. 346*, 767−776.
48. Xia, Y., Dawson, V. L., Dawson, T. M., Snyder, S. H., and Zweier, J. L. (1996) *Proc. Natl. Acad. Sci. U.S.A. 93*, 6770−6774.
49. Abu-Soud, H. M., Wang, J., Rousseau, D. L., Fukuto, J. M., Ignarro, L. J., and Stuehr, D. J. (1995) *J. Biol. Chem. 270*, 22997−23006.
50. Abu-Soud, H. M., Rousseau, D. L., and Stuehr, D. L. (1996) *J. Biol. Chem. 271*, 32515−32518.
51. Hines, R. N., and Prough, R. A. (1980) *J. Pharmacol. Exp. Ther. 214*, 80−86.
52. Vasquez-Vivar, J., Martasek, P., Hogg, N., Masters, B. S. S., Pritchard, K. A., and Kalyanaramn, B. (1997) *Biochemistry 36*, 11293−11297.
53. Abu-Soud, H. M., Feldman, P. L., Clark, P., and Stuehr, D. J. (1994) *J. Biol. Chem. 269*, 32318−32326.
54. Griscavage, J. M., Fukuto, J. M., Komori, Y., and Ignarro, L. J. (1994) *J. Biol. Chem. 269*, 21644−21649.
55. Foote, C. S. (1994) *Toxicol. Lett. 93*, 29−44.
56. Chabin, R. N., McCauler, E., Calaycay, J. R., Kelly, T. M., MacNaul, K. L., Wolfe, G. C., Hutchinson, N. I., Madhusudanaraju, S., Schmidt, J. A., Kozarich, J. W., and Wong, K. K. (1996) *Biochemistry 35*, 9567−9575.
57. Mayer, B., Klatt, P., Werner, E. R., and Shmidt, K. (1994) *FEBS Lett. 350*, 199−202.

BI0019444